



## On the Carbon Solubility in Expanded Austenite and Formation of Hägg Carbide in AISI 316 Stainless Steel

Christiansen, Thomas Lundin; Ståhl, Kenny; Brink, Bastian; Somers, Marcel A. J.

*Published in:*  
Steel Research International

*Link to article, DOI:*  
[10.1002/srin.201500415](https://doi.org/10.1002/srin.201500415)

*Publication date:*  
2016

*Document Version*  
Peer reviewed version

[Link back to DTU Orbit](#)

*Citation (APA):*  
Christiansen, T. L., Ståhl, K., Brink, B., & Somers, M. A. J. (2016). On the Carbon Solubility in Expanded Austenite and Formation of Hägg Carbide in AISI 316 Stainless Steel. *Steel Research International*, 87(11), 1395–1405. <https://doi.org/10.1002/srin.201500415>

---

### General rights

Copyright and moral rights for the publications made accessible in the public portal are retained by the authors and/or other copyright owners and it is a condition of accessing publications that users recognise and abide by the legal requirements associated with these rights.

- Users may download and print one copy of any publication from the public portal for the purpose of private study or research.
- You may not further distribute the material or use it for any profit-making activity or commercial gain
- You may freely distribute the URL identifying the publication in the public portal

If you believe that this document breaches copyright please contact us providing details, and we will remove access to the work immediately and investigate your claim.

# On the Carbon Solubility in Expanded Austenite and Formation of Hägg Carbide in AISI 316 Stainless Steel.

Thomas L. Christiansen<sup>1\*</sup>, Kenny Ståhl<sup>2</sup>, Bastian K. Brink<sup>1</sup> and Marcel A.J. Somers<sup>1</sup>

<sup>1</sup> *Department of Mechanical Engineering, DTU, Produktionstorvet, DK-2800 Kgs. Lyngby*

<sup>2</sup> *Department of Chemistry, DTU, Kemitorvet, DK-2800 Kgs. Lyngby*

\*corresponding author: [tch@mek.dtu.dk](mailto:tch@mek.dtu.dk)

## Abstract

The carbon solubility in expanded austenite was investigated by controlled low temperature gaseous *through*-carburizing of AISI 316 stainless steel thin foils with thermogravimetry and synchrotron powder diffraction analysis. Carburizing was carried out in C<sub>2</sub>H<sub>2</sub>-H<sub>2</sub>-N<sub>2</sub> and CO-H<sub>2</sub>-N<sub>2</sub> atmospheres at 380-420°C and 465-470°C, respectively. Hägg carbide ( $\chi$ -M<sub>5</sub>C<sub>2</sub>) develops when the carbon content in the expanded austenite exceeds the metastable solubility limit; the transformation of carbon expanded austenite into Hägg carbide occurs *irrespective* of carburizing temperature in the investigated temperature range (380-470°C). The maximum solubility of carbon in expanded austenite (380°C) was found to correspond to an occupancy ( $y_C$ ) of 0.220 of the interstitial octahedral sites of the austenite lattice (i.e. 4.74 wt% C). Decomposition of Hägg carbide into M<sub>7</sub>C<sub>3</sub> occurred upon prolonged carburizing treatment or thermal exposure in inert atmosphere (in-situ synchrotron experiments).

## Keywords

Carbon solubility; expanded austenite; thermogravimetry; synchrotron diffraction; Hägg carbide.

## 1. Introduction

Carburizing of stainless steel at temperatures below 550°C can result in the development of a surface zone consisting of a supersaturated solid solution of interstitially dissolved carbon atoms, so

called carbon expanded austenite. Up to about 550 °C carbon expanded austenite is considered to be kinetically stabilized within the usual treatment time by the sluggish development of the more stable chromium carbides. Analogously, nitrogen expanded austenite can be obtained by nitriding, albeit at temperatures approximately 100 °C degrees lower, i.e. typically below 450°C, because the driving force for chromium nitride formation is larger than for chromium carbide formation.<sup>[1]</sup> Carbon expanded austenite “layers” can be obtained by different techniques, including gas, plasma and salt-bath carburizing.<sup>[1,2 3,4,5]</sup> Transformation of the surface of stainless steel into carbon (or nitrogen) expanded austenite is associated with highly beneficial properties with respect to wear and corrosion.

Carbon has a strong affinity to chromium and EXAFS studies of pure carbon expanded austenite in AISI 316 with a carbon content of 2.5 wt.% (equivalent to an interstitial occupancy,  $y_C$ , of 0.115<sup>[1]</sup>) obtained by carburizing at 420°C, indeed show that carbon atoms reside in the immediate vicinity of chromium atoms without forming carbides, implying that short range ordering of Cr and C occurs.<sup>[6]</sup> Analogous observations were previously reported for Cr and N in nitrogen expanded austenite.<sup>[7]</sup>

The maximum carbon solubility in expanded austenite has so far not been assessed, as opposed to the nitrogen solubility. The topic of carbon solubility in expanded austenite has been addressed e.g. in refs.<sup>[8,9, 10]</sup> for gas and plasma carburizing. For gas carburizing Michal et al.<sup>[8]</sup> reported an experimental carbon solubility of up to 12 at.% ( $y_C = 0.136$ ); for plasma carburizing Sun et al.<sup>[10]</sup> obtained 3 wt % ( $y_C = 0.138$ ). It is important to realize that these consistent values for the carbon solubility were obtained in heterogeneous samples where an expanded austenite case is present on a carbon free core. Consequently, expanded austenite is under a state of compressive stress and a carbon concentration profile over the case maintains inward diffusion of carbon to promote further growth of the expanded austenite zone.

---

<sup>i</sup>  $y_C$  is equivalent to the number of carbon atoms per metal atom for an f.c.c. lattice; this is directly converted into atomic percent, i.e.  $X_C = y_C / (1 + y_C)$ .

Few data exist on homogenous, through-carburized expanded austenite samples. A maximum carbon content of 3.36 wt.% ( $y_C = 0.156$ ) was obtained in homogenous and stress-free carbon expanded austenite in ref.<sup>[9]</sup> In this work AISI 316 stainless steel foils were carburized at 420°C to different overall carbon contents and subsequently homogenized in an inert atmosphere at 500°C for 5 hours to obtain a uniform carbon distribution over the foil thickness. No information for carbon contents in excess of 3.36 wt.% ( $y_C = 0.156$ ) have so far been reported.

Development of  $\chi$ -  $M_5C_2$  carbide, isomorphic with Hägg carbide, and in the sequel referred to as Hägg carbide, has been reported in low temperature carburized stainless steel AISI 316.<sup>[11,12,13,14]</sup> Hägg carbide has a triclinic structure (P-1) with one C atom and three crystallographically independent M atoms in the asymmetric unit.<sup>[15]</sup> The occurrence of Hägg carbide was observed in both bulk, foil and powder samples of AISI 316 after repeated cycles in a gaseous carburizing process using CO-H<sub>2</sub>-N<sub>2</sub> atmospheres (44 to 246 hours at 465-470°C).<sup>[11,12]</sup>

The present investigation addresses carbon solubility in stainless steel AISI 316 (through)-carburized under controlled conditions in CO-H<sub>2</sub>-N<sub>2</sub> and C<sub>2</sub>H<sub>2</sub>-H<sub>2</sub>-N<sub>2</sub> atmospheres at low temperatures. A thermogravimetric approach, previously used in ref.<sup>[16]</sup> for determination of the nitrogen solubility in expanded austenite, is adopted.

## **2. Experimental**

### **2.1. Gaseous carburizing**

Stainless steels, 5- $\mu$ m-thick AISI 316 powder and 7.5- $\mu$ m-thick AISI 316 foil with nominal composition Fe/Cr18/Ni10/Mo3 (wt.%) were applied in the investigation. The 7.5  $\mu$ m foil was purchased from Goodfellow and the 5  $\mu$ m (spray atomized) powder was provided by Höganäs AB.

The foil was austenitized at 1080°C in an atmosphere of flowing hydrogen (99.999%). The 5 µm powder was not austenitized prior to low temperature carburizing to prevent unwanted sintering. The powder contained a minor fraction of delta ferrite. The application of 7.5-µm-thin foils and 5 µm powder should facilitate fast establishment of metastable equilibrium between gaseous atmosphere and solid state, i.e. it is possible to obtain virtually *homogenous* carbon contents throughout the entire thickness of the material. This implies that the influence of composition gradients and residual stresses on the phase stability and carbon solubility can be excluded. Fast *through-carburizing* was experimentally verified by light optical microscopy for a range of different thicknesses for powder and foil of AISI 316 stainless steel (not shown here).

The AISI 316 foil was activated for carburizing by replacing the passive film with an electrodeposited Ni-layer of several nanometers thickness (cf. the patented method described in ref.<sup>[17]</sup>). The thin Ni layer is penetrable for carbon atoms, prevents repassivation and is effective in catalyzing the decomposition of the CO molecule, and thus promotes the carburizing reaction. For the low temperature regime (see below) the 5 µm powder was applied using the method described in ref.<sup>[18]</sup>

All gaseous carburizing treatments were performed in (two) ceramic crucibles which were mounted directly on the internal thermocouples in a Netzsch Thermal analyzer STA449, thereby enabling continuous monitoring of the total carbon uptake. The advantage of using thin foils/powder is a high packing factor in the crucibles of the thermobalance and consequently a high surface area to weight ratio which gives an excellent resolution on the recorded mass-uptake curve, provided that soot formation does not take place. The 7.5 µm foils were carburized in an atmosphere consisting of 36%CO-55%H<sub>2</sub>-9%N<sub>2</sub> (vol.%) and 9%CO-45%H<sub>2</sub>-46%N<sub>2</sub> at 465°C and 470°C, respectively.<sup>[ii]</sup> The

---

<sup>ii</sup> N<sub>2</sub> was required for the thermobalance in order to protect the balance electronics and have stable flow condition in the measuring compartment.

durations of the carburizing treatments were 1257 minutes and 5939 minutes, for 465°C and 470°C, respectively. Incidentally soot formation was observed on the 7.5 µm foils carburized at 470°C in one of the two crucibles used; no soot formation was observed on the 7.5 µm foils carburized at 465°C. For the 7.5 µm sample carburized at 465°C the CO content in the gas was reduced after a sudden increase of the carbon uptake was observed after an extended period of carburizing; in the last step the atmosphere was changed to H<sub>2</sub> (+N<sub>2</sub>).

In order to assess the solubility of carbon in AISI 316 stainless steel at a lower temperature regime the use of another carburizing medium is required. The gas mixtures applied at temperatures 465-470°C are not applicable for lower temperatures. Mixtures of acetylene-hydrogen can be used at low temperatures as the tendency for soot formation is strongly mitigated (acetylene is highly unstable and has a strong propensity for developing soot, e.g. at 470°C). In principle, the carbon activity can be straightforwardly derived from the partial pressure of hydrogen and acetylene (which is not the case for CO-H<sub>2</sub> gas mixtures<sup>[1]</sup>). The use of acetylene allows the use of powder materials as no ex-situ surface activation is required; instead surface activation is achieved directly in acetylene.<sup>[18]</sup>

The 5 µm powder was carburized in an atmosphere of 2% C<sub>2</sub>H<sub>2</sub>-89% H<sub>2</sub>-9% N<sub>2</sub> at 380°C, 400 and 420°C for 4140, 2500 and 1408 minutes, respectively (the durations reflect that a stationary state was obtained). An additional sample, for *in situ* investigation of thermal decomposition, was produced by carburizing at 420°C for 240 minutes followed by continued carburization for 960 minutes at 400°C.

## 2.2. Synchrotron and X-ray powder diffraction

Synchrotron powder diffraction was performed in transmission mode with a HUBER G670 Guinier camera at MAX-lab beamline I711.<sup>[19]</sup> The (brittle) sample foils/powder were mounted with two pieces of tape and eight Al foils (total thickness 160 µm) were placed between sample and detector

to reduce the contribution of fluorescence radiation. Wavelengths of  $\lambda=1.07198(1)$  Å and  $1.00195(1)$  Å were used to have access to an extended range of Bragg peaks. Each sample was rotated during 2 min measurements using a beam size of  $0.3 \times 1.0$  mm. The data was corrected for  $2\theta$  zero-shift as determined for a Si standard along with the actual wavelength and the instrumental broadening as well as for the  $45^\circ$  Guinier tangent angle. For the *in situ* investigation, the powder sample was mounted in a 0.7 mm inner diameter quartz capillary filled with an inert argon atmosphere to avoid oxidation and heated in a Huber 670.3 furnace. Diffraction data were recorded with a wavelength of  $\lambda = 1.07051(2)$  Å at 26 temperatures steps in the range 110 – 650°C with an exposure time of 240 seconds at each step. After exposure, the temperature was immediately ramped to the next set point, and the average time for reaching and stabilizing at each set point temperature prior to exposure was 205 seconds.

X-ray diffraction (XRD) data was collected using a Bruker D8 AXS diffractometer equipped with a Cu anode and a Göbel mirror in the incident beam operating in Bragg-Brentano mode. A step-size of  $0.02^\circ$  and a (long) step-time of 57.3 seconds were applied. All diffractograms were obtained at room temperature.

Rietveld refinements were performed of (synchrotron) X-ray diffraction results using a modified version of the LHMP1 Rietveld program.<sup>[20]</sup> The outcome of the Rietveld refinements were the constituent phases, their lattice parameters and their corresponding mass fractions. Atomic positions were not refined and stoichiometric compositions were assumed for the carbides using the following crystal structures as initial models:  $\text{Fe}_3\text{C}$ <sup>[21]</sup>,  $\text{M}_5\text{C}_2$ <sup>[22]</sup>,  $\text{M}_7\text{C}_3$ <sup>[23]</sup> and  $\text{M}_{23}\text{C}_6$ <sup>[24]</sup>

### 3. Results and interpretation

#### 3.1. Thermogravimetry

### 3.1.1. CO-H<sub>2</sub>-N<sub>2</sub> carburizing atmosphere (465/470°C)

Carbon uptake during carburizing of 7.5 µm thin foils of AISI 316 is shown in Figure 1 for the two different carburizing conditions.

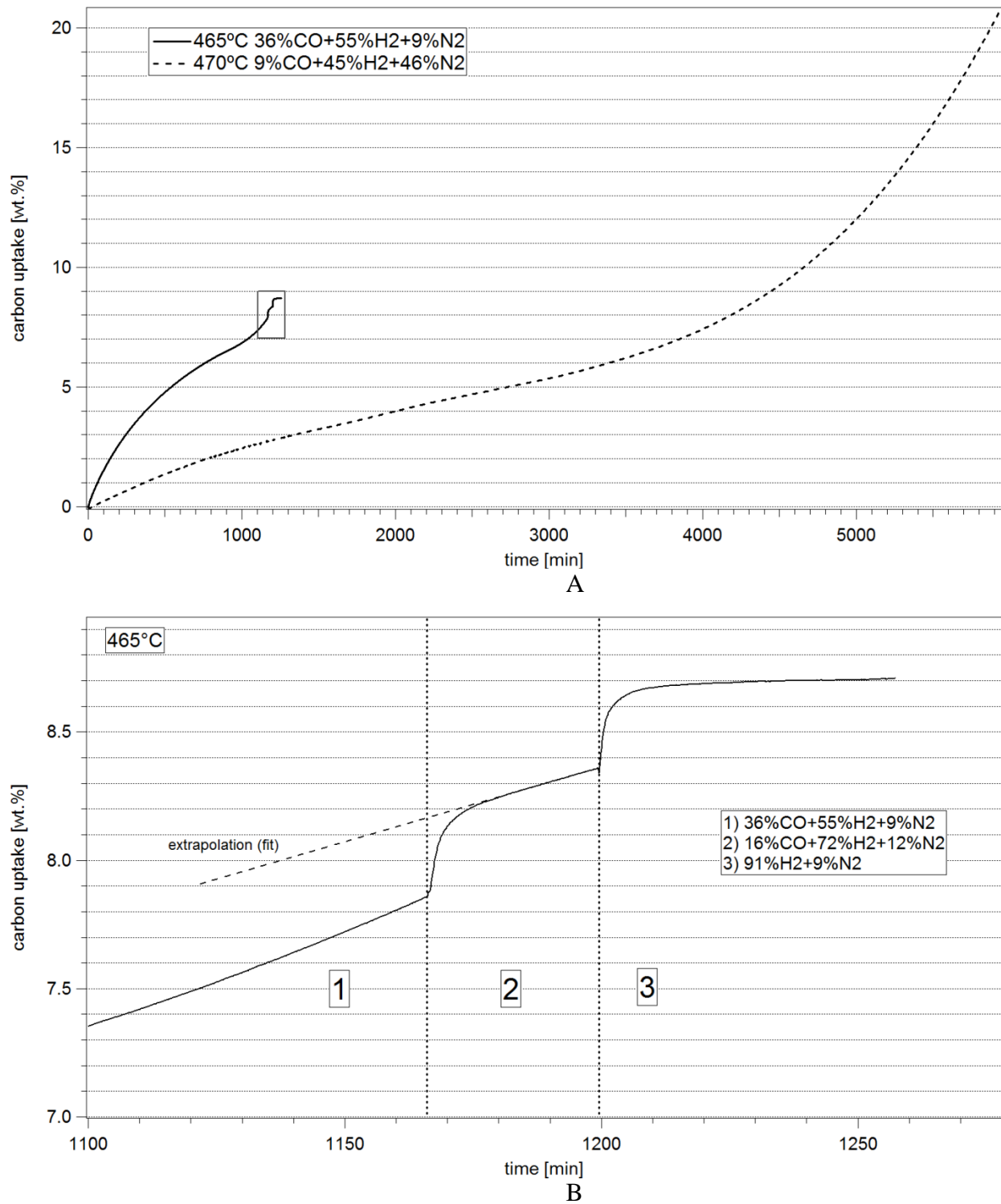


Figure 1. Thermogravimetry. CO-H<sub>2</sub>-N<sub>2</sub> carburizing of 7.5 µm foils. Figure B is an enlargement of the last part (boxed) of the thermogravimetric curves for the 465°C carburizing treatment given in A.

Initially, the sample carburized in 36% CO at 465°C has a fast uptake of carbon. When a carbon content of approximately 6 wt% is reached an increase in mass-uptake rate is observed, implying that equilibrium between the gas atmosphere and the foils is not attainable under these conditions and that a transformation occurs whereby the capacity for carbon accommodation is enhanced. The last part (boxed) of the uptake curve is enlarged in Figure 1B. During the investigations the increase in carbon uptake occurring at around 6 wt.% C (after approximately 800 minutes) was interpreted as development of soot at the sample surface resulting from a (too) high carbon activity in the gas. Therefore the amount of CO in the gas was reduced in order to lower the carbon activity<sup>[iii]</sup>; this corresponds to regime 2 in Figure 1B. The abrupt change in uptake between regions 1 and 2 is caused by a change in buoyancy due to an altered gas composition and is hence not related to the carbon uptake in the sample. Clearly, reducing the CO content in the gas mixture did not change the rate of carbon uptake significantly, evidenced by a slightly reduced slope in the uptake curves in region 1 and 2 in Fig. 1B (compare the uptake curve in regime 1 with the extrapolated line fitted to the uptake curve from regime 2) . The last step, regime 3 in Figure 1B, corresponds to a fully reducing atmosphere of flowing hydrogen, i.e. without CO. Flowing hydrogen brings the uptake of carbon to a halt as evidenced by the horizontal uptake curve. Interestingly, for such high carbon contents no weight *decrease* is observed in flowing hydrogen, indicating that no carbon is retracted from the material. This behavior has the implication that 1) carbon atoms are more strongly bound in the solid state than in hydrocarbons and/or 2) the surface kinetics involved in forming hydrocarbons is too slow for a significant retraction to take place. Retraction of carbon atoms by hydrogen would entail the formation of methane CH<sub>4</sub>, which formation indeed is expected to be slow in this temperature range.<sup>[25]</sup>

The foils carburized at 470°C were exposed to a gas mixture with a lower content of CO and higher amount of inert N<sub>2</sub> to circumvent the (unwanted) sudden increase in uptake at a carbon content of 6

---

<sup>iii</sup> Strictly speaking, the carbon activity cannot directly be related to the amount of CO in the gas unless the water vapor content is known.

wt%. The amount of inert nitrogen was increased to mitigate the tendency for soot formation. The initial uptake of carbon with a low CO content is not as fast as for the atmosphere with a high CO content, which is attributed to a lower applied chemical potential of carbon and a concomitant lower driving force for growth of the carbon expanded austenite zone. However, when a carbon content of approximately 5 wt% is reached (after approximately 4000 minutes) the uptake increases, analogous to the 465°C high-CO uptake curve. The last part of the uptake is characterized by a very steep increase which could be attributed to soot formation on the samples (a slight amount of soot was indeed observed to have formed in one of the two crucibles where the samples were positioned). The lower content of CO clearly postpones (in time) the onset of the sudden increase in uptake. As the foils are relatively thin and the growth rate of the expanded austenite layer is relatively fast, through-carburizing of the foils is expected to occur within a few hours of carburizing. At this point it is expected that the composition-induced stresses (either compressive or tensile) are largely alleviated due to a uniform carbon concentration throughout the foil. Evidently, for neither of the carburizing conditions can a metastable equilibrium be obtained between the carbon expanded austenite in the foils and the imposed carbon activity in the gas atmosphere for the applied temperature regime. Such metastable equilibrium *is* attainable for the nitrogen expanded austenite system.<sup>[26]</sup>

### **3.1.2. C<sub>2</sub>H<sub>2</sub>-H<sub>2</sub>-N<sub>2</sub> carburizing atmosphere (420 - 380°C regime)**

The carbon uptake curves for carburizing of 5 µm AISI 316 powder in a C<sub>2</sub>H<sub>2</sub>-H<sub>2</sub>-N<sub>2</sub> gas atmosphere at 380, 400 and 420°C are shown in Figure 2.

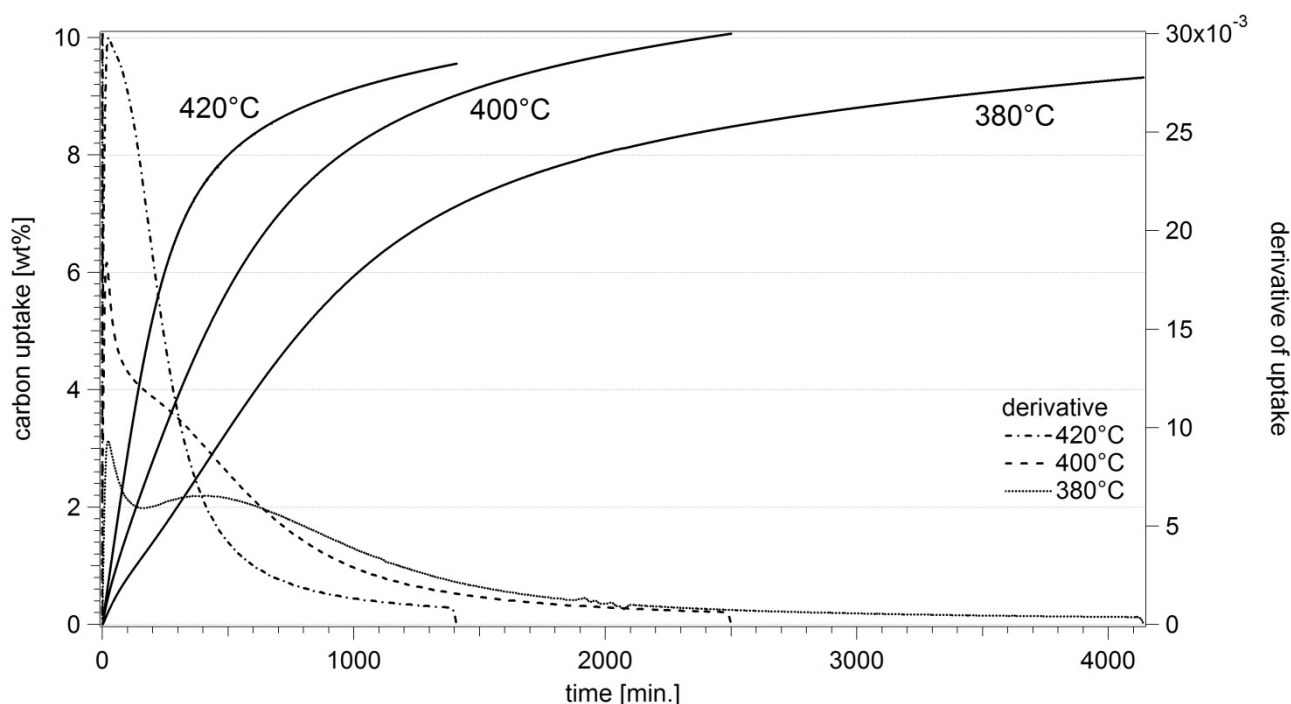


**Figure 2. Thermogravimetry. Carburizing of 5  $\mu\text{m}$  powder in an acetylene atmosphere at the temperatures 380°C, 400°C and 420°C.**

Obviously, acetylene is a highly potent carburizing agent as a high carbon content is rapidly obtained at all temperatures which can be attributed to the high carbon activity imposed by acetylene (triple unsaturated hydrocarbon compound) and the ostensibly fast surface kinetics as compared to carburizing in CO (despite the catalyzing influence of the Ni film on CO dissociation). The effect of carburizing temperature is obvious as the uptake slows down as the carburizing temperature is lowered. The shape of the uptake curves is largely identical: an initially fast increase in carbon uptake which slows down and enters into a steady-state regime exhibiting linear kinetics. The derivative of all uptake curves eventually becomes constant and larger than nil, which means that a metastable equilibrium between gas and solid state is not attained within the time frame of these experiments. However, within the carburizing time-span, the uptake curves do not exhibit a sudden increase in uptake as was observed for the CO-carburizing uptake curves in Figure 1. For the 380°C curve an increase in uptake rate is observed after approximately 150 minutes and the same trend can also be observed at 400°C (see the derivative curves in Figure 2). After carburizing the powder had a dark appearance, but no soot formation, could be observed. An overall carbon uptake of more than 9 wt% is achieved, provided that all carbon is taken up by the powder.

## 3.2. Powder diffraction analysis

### 3.2.1. CO-H<sub>2</sub>-N<sub>2</sub> carburizing atmosphere (465/470°C)

Phase analysis of the CO carburized 7.5  $\mu\text{m}$  thin foils was investigated with synchrotron powder diffraction; the diffractograms are given in Figure 3. Results of the Rietveld refinements of the diffractograms are collected in Table 1.

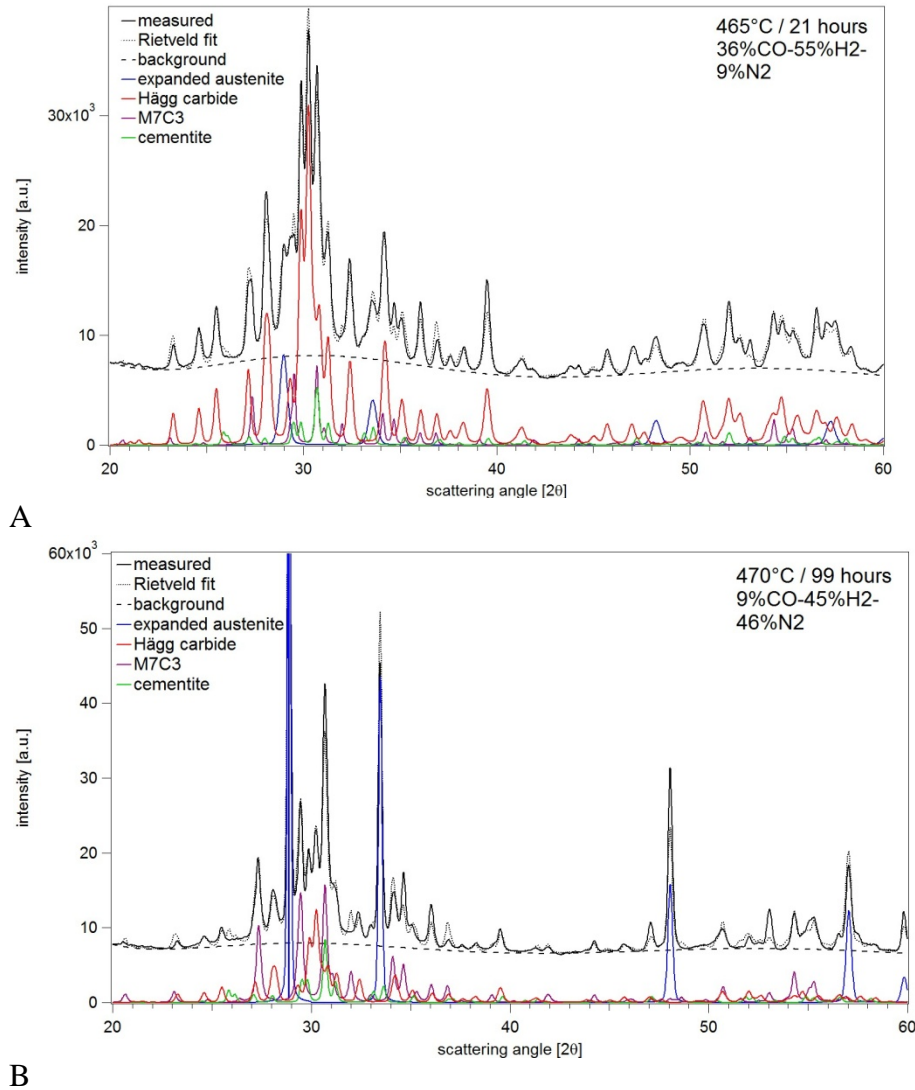


**Figure 3.** Synchrotron powder diffraction ( $\lambda=1.07198(1)$  Å) and Rietveld refinements of CO-H<sub>2</sub>-N<sub>2</sub> carburized 7.5  $\mu\text{m}$  foils (cf. Figure 1) A) 465°C and B) 470°C. Experimental details are indicated in the graphs. Please notice that the (111)  $\gamma_C$  peak reflection (at 29°) for the 470°C / 99 hours sample is not fully contained within the applied range on the ordinate axis.

**Table 1. Rietveld refinements (CO-H<sub>2</sub>-N<sub>2</sub> carburizing) - synchrotron powder diffraction ( $\lambda=1.07198(1)$  Å).**

<b>465°C sample</b>					
Phase	M <sub>7</sub> C <sub>3</sub>	M <sub>5</sub> C <sub>2</sub>	M <sub>23</sub> C <sub>6</sub>	Fe <sub>3</sub> C	$\gamma_C$
Space group	Pnma	P -1	Fm3m	Pnma	Fm3m
<i>a</i> [Å]	4.4915 (0.00060)	11.5998 (0.00084)	-	5.068 (0)	3.7095 (0.00035)
<i>b</i> [Å]	6.934 (0.0017)	4.5661 (0.00035)	-	6.767 (0)	-
<i>c</i> [Å]	11.995 (0.0031)	5.0775 (0.00041)	-	4.560 (0)	-
$\beta$ [°]	-	97.765 (0)	-	-	-
Mass fraction [wt. %]	11.5 (0.2)	73.1 (0.8)	0	7.4 (0.2)	8.0 (0.2)
<b>470°C sample</b>					
<i>a</i> [Å]	4.5009 (0.00059)	11.609 (0.0023)	10.691 (0.0059)	5.056 (0.0020)	3.7227 (0.00018)
<i>b</i> [Å]	6.931 (0.0018)	4.5630 (0.00097)	-	6.773 (0.0023)	-
<i>c</i> [Å]	12.002 (0.0036)	5.077 (0.0010)	-	4.575 (0.0016)	-
$\beta$ [°]	-	97.765 (0)	-	-	-
Mass fraction [wt. %]	30.2 (0.6)	25.3 (0.5)	1.5 (0.2)	9.4 (0.4)	33.6 (0.4)

The foils consist of a mixture of carbon expanded austenite, M<sub>7</sub>C<sub>3</sub>, cementite Fe<sub>3</sub>C and Hägg carbide M<sub>5</sub>C<sub>2</sub>. The foil carburized at 465°C for 21 hours in the CO-rich gas mixture is almost fully transformed into Hägg carbide (and minor fractions of M<sub>7</sub>C<sub>3</sub> and Fe<sub>3</sub>C). The duration of only 21 hours at 465°C for the formation of Hägg carbide is unprecedentedly short as compared to reported observations of Hägg carbide in austenitic stainless steel (cf. introduction). According to the Rietveld refinement a minor fraction of only 8.0 mass % of the sample consists of carbon expanded austenite. The lattice parameter obtained for the remaining carbon expanded austenite corresponds to  $y_C=0.187$  (4.04 wt% C), provided that the relationship between the lattice parameter and carbon content in ref.<sup>[9]</sup> can be extrapolated to higher C contents.

The sample carburized at 470°C with a low content of CO also consists of a mixture of carbon expanded austenite,  $M_7C_3$ ,  $Fe_3C$  and Hägg carbide (and a very small fraction of  $M_{23}C_6$ ). However, the phase fractions of expanded austenite and  $M_7C_3$  are significantly higher than for the high CO experiment. The carbon content in the expanded austenite is slightly higher than for the sample carburized at 465°C, here a carbon content of  $y_C=0.209$  (4.51 wt% C) is obtained. Even though the duration of the 470°C carburizing treatment is appreciably longer than the 465°C carburizing treatment, it appears that the development of Hägg carbide is not so prominent. This indicates that carbides first develop above a critical carbon concentration; cf. the sudden increase in uptake at 5-6 wt.% carbon (Figure 1).

### 3.2.2. $C_2H_2-H_2-N_2$ carburizing atmosphere (420-380°C regime)

The synchrotron powder diffraction pattern for the powder carburized in acetylene at 380°C is given in Figure 4 and the results of the Rietveld refinements are given in Table 2.

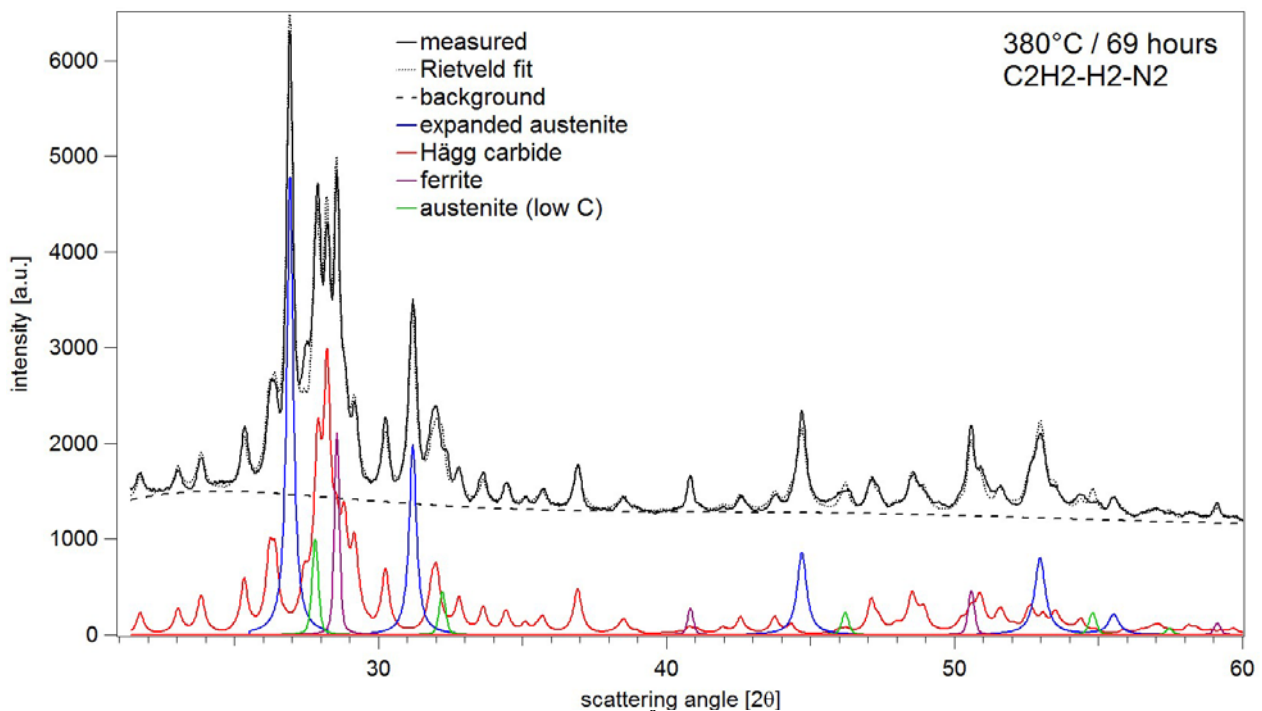


Figure 4. Synchrotron powder diffraction ( $\lambda=1.00195(1)$  Å) and Rietveld refinements of carburised 5  $\mu m$  powder. Carburized at 380°C in acetylene (see corresponding TGA curve in Figure 2).

**Table 2. Rietveld refinements (acetylene carburizing at 380°C) - synchrotron powder diffraction ( $\lambda=1.00195(1)$  Å).**

Phase	$\gamma_{C,low}$	$\gamma_{C,high}$	$M_5C_2$	Ferrite, $\alpha$
Space group	Fm3m	Fm3m	P -1	Im3m
$a$ [Å]	3.6108 (0.00035)	3.7259 (0.00027)	11.613 (0.0011)	2.8720 (0.00021)
$b$ [Å]	-	-	4.5670 (0.00049)	-
$c$ [Å]	-	-	5.0621 (0.00051)	-
$\beta$ [°]	-	-	97.803 (0)	-
Mass fraction [wt.%]	4.2 (0.1)	26.0 (0.3)	64.5 (0.7)	5.3 (0.1)

The powder consists of a mixture of carbon expanded austenite, Hägg carbide and a minor fraction of untransformed delta ferrite that was initially present in the powder because it was not austenitized prior to carburizing to avoid sintering. The observations of carbon expanded austenite and Hägg carbide are consistent with CO carburizing at higher temperatures. Interestingly, no formation of  $M_7C_3$  (or  $Fe_3C$ ) was observed. The carbon content in expanded austenite is higher compared to the foil material carburized with CO, which can be attributed to a higher solubility at lower temperature and/or a higher effective carbon activity in the gaseous phase. The relatively low carburizing temperature still gives rise to massive formation of Hägg carbide. According to Rietveld refinements 64% of the sample consists of Hägg carbide. The carbon expanded austenite was in the Rietveld refinements described by two different austenite peaks with different interstitial contents,  $\gamma_{C,high}$  and  $\gamma_{C,low}$ , in order to correctly describe the slight asymmetry resulting from inhomogeneities in carbon content. It cannot be excluded that this has a physical meaning, but it is merely a pragmatic way of handling variations in carbon content to obtain convergence in the refinement. The maximum carbon content in the expanded austenite based on the lattice expansion is  $y_C = 0.215$  (4.65 wt.%).

X-ray diffraction patterns of all acetylene carburized samples are shown in Figure 5 together with Rietveld refinements; the results of the Rietveld refinements are given in Table 3.

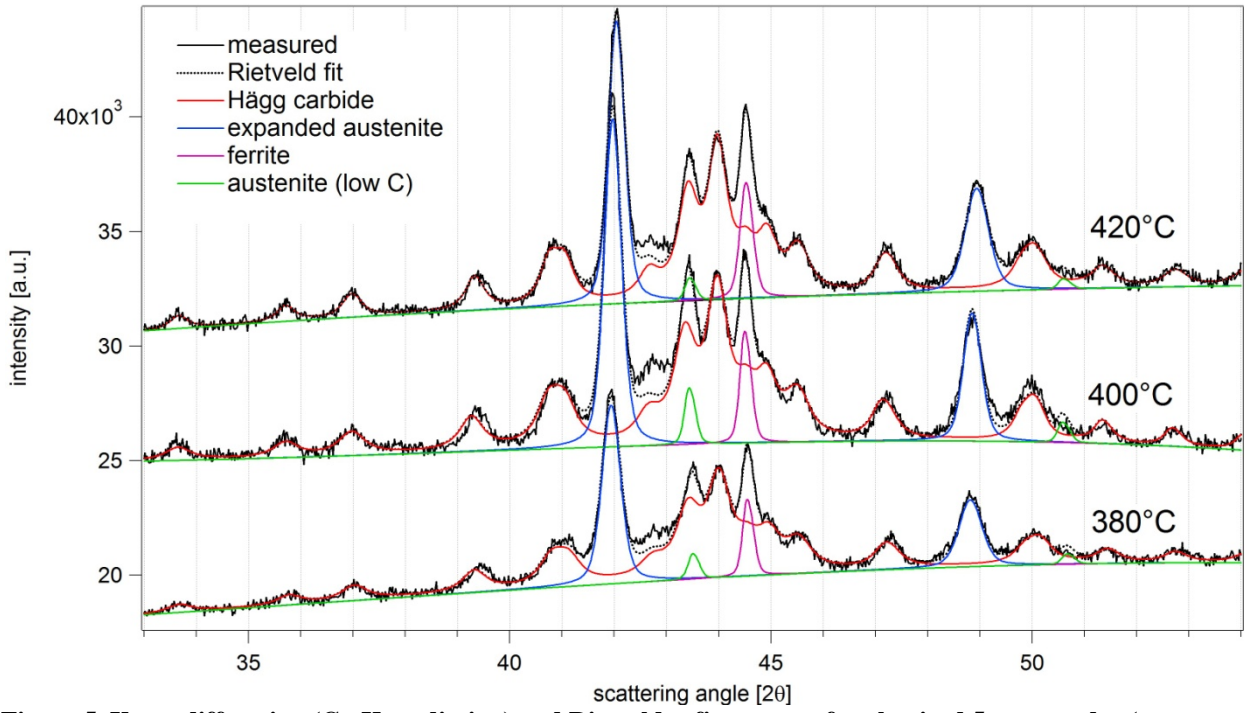


Figure 5. X-ray diffraction (Cu  $K_\alpha$  radiation) and Rietveld refinements of carburized 5  $\mu\text{m}$  powder (see corresponding TGA curves in Figure 2). All carburizing temperatures result in massive formation of Hägg carbide  $\text{M}_5\text{C}_2$ .

Table 3. Rietveld refinements (acetylene carburizing 380-420°C) - X-ray diffraction (Cu  $K_\alpha$  radiation).

Phase	$\gamma_{\text{C,low}}$	$\gamma_{\text{C,high}}$	$\text{M}_5\text{C}_2$	Ferrite, $\alpha$
Space group	Fm3m	Fm3m	P -1	Im3m
<b>380°C</b>				
$a$ [Å]	3.601 (0.0021)	3.731 (0.0021)	11.623 (0.0067)	2.875 (0.0016)
$b$ [Å]	-	-	4.582 (0.0027)	-
$c$ [Å]	-	-	5.067 (0.0031)	-
$\beta$ [°]	-	-	97.803 (0)	-
Mass fraction [wt.%]	1.9 (0.2)	22 (2)	72 (7)	4.0 (0.5)
<b>400°C</b>				
$a$ [Å]	3.607 (0.0017)	3.728 (0.0017)	11.627 (0.0055)	2.878 (0.0013)
$b$ [Å]	-	-	4.588 (0.0023)	-
$c$ [Å]	-	-	5.074 (0.0026)	-
$\beta$ [°]	-	-	97.74 (0.022)	-
Mass fraction [wt.%]	2.7 (0.3)	24 (2)	69 (5)	4.1 (0.4)
<b>420°C</b>				
$a$ [Å]	3.606 (0.0017)	3.722 (0.0014)	11.629 (0.0044)	2.877 (0.0011)
$b$ [Å]	-	-	4.581 (0.0018)	-
$c$ [Å]	-	-	5.074 (0.0021)	-
$\beta$ [°]	-	-	97.74 (0.015)	-
Mass fraction [wt.%]	1.2 (0.1)	24 (1.5)	70 (4)	5.4 (0.4)

The line profiles are largely identical, i.e. they all contain a high fraction of Hägg carbide of around 70 wt.% (commensurate with synchrotron results) and  $\text{M}_7\text{C}_3$  is not observed. For all graphs in Figure 5 a discrepancy is observed between the measured profile and the fitted profile at 42.8°

(similarly in Figure 4 at 27.5°). It is not clear whether this can be attributed to i) the presence of ferrite in the powder, which upon carburizing dissolves carbon and becomes tetragonally distorted (expanded martensite), ii) a gradient in the carbon content in expanded austenite or iii) an inaccurate crystallographic description of Hägg carbide.

### 3.2.3. Thermal decomposition

For the powder sample used for the *in situ* investigation of thermal decomposition, phase composition versus temperature up to 650°C is shown in Figure 6.

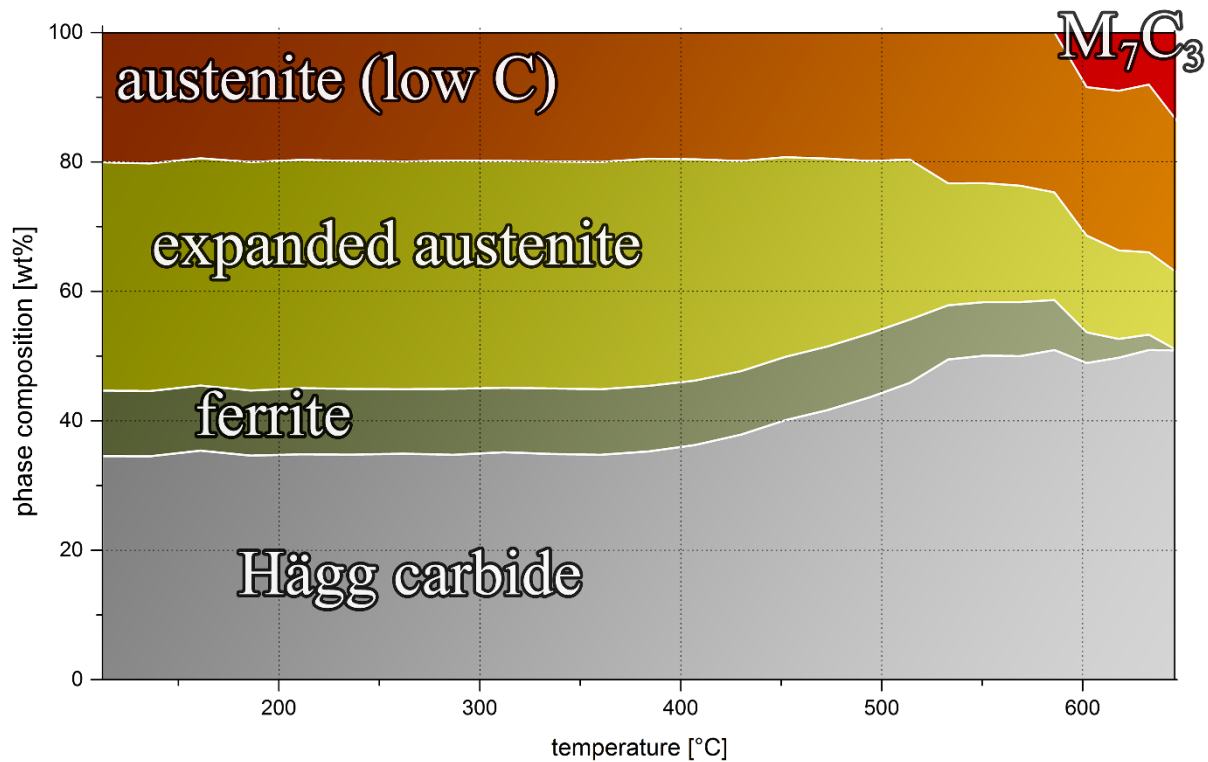


**Figure 6.** Phase transformation map, i.e. phase composition versus temperature for carburized 5 μm powder initially composed of expanded austenite, austenite (low C), ferrite and Hägg carbide ( $M_5C_2$ ). Estimated standard deviations from Rietveld refinements are  $\leq 1.5$  wt%.

The initial constituent phases are similar to the previous carburized powder samples; expanded austenite, austenite (low C) and Hägg carbide. Based on lattice expansion, the initial carbon content in the expanded austenite is  $y_C = 0.219$ . The lower content of Hägg carbide (35 wt%) compared to the previous powder samples is consistent with a shorter carburizing time at 400°C. It is evident from Figure 6 that expanded austenite decomposes above 390°C, which causes additional formation

of Hägg carbide. Above 600°C the  $M_7C_3$  carbide is formed along with the disappearance of ferrite on reaching 650°C. During decomposition of expanded austenite, the lattice parameter gradually decreases due to the decreasing interstitial carbon content as a consequence of Hägg carbide formation (not shown). This behavior is similar to that of nitrogen expanded austenite.<sup>[22]</sup>

## 4. Discussion

### 4.1. Carbon solubility and homogeneity range of carbon expanded austenite

Synchrotron powder diffraction data shows that expanded austenite has a lattice parameter of up to 3.7292 Å (X-ray diffraction: 3.731 Å) which corresponds to a maximum solubility of  $y_C=0.220$  at 380°C and a slightly lower solubility at 465-470°C. The upper limit in the homogeneity range of expanded austenite is defined by this carbon content at this specific temperature and carbon activity. It should be noted that the carbon activity for the applied gas composition<sup>[iv]</sup> at 380°C is  $5.75 \cdot 10^5$ , which is extremely high. It should also be emphasized that the obtained maximum carbon solubility in expanded austenite is obtained under the co-existence of Hägg carbide. The lattice parameter of the expanded austenite increases slightly when the carburizing temperature is lowered (Table 3), which can be attributed to a temperature dependence on the carbon solubility in the expanded austenite and/or a slightly higher carbon activity in the gas phase at lower temperatures (provided that local equilibrium is attained). Comparison of the carbon expanded austenite system with the analogous nitrogen expanded austenite system clearly shows dissimilarities: 1) The maximum solubility of carbon in expanded austenite is lower than for nitrogen in (nitrogen) expanded under similar conditions. This is not unexpected as the affinity of chromium to nitrogen is stronger than to carbon. 2) The carbon expanded austenite systems transform into a metastable iron-based carbide phase (Hägg carbide) upon exceeding a certain interstitial content; this behavior is not observed for the nitrogen expanded austenite system. Even for imposed conditions of infinitely high nitrogen activity (pure ammonia) nitrogen expanded austenite is found to be in metastable equilibrium, i.e. it

---

<sup>iv</sup> Provided that thermal decomposition of acetylene in the gas phase is negligible.

does not undergo transformation into iron-based nitrides. Rather chromium-based nitrides develop, which is associated with decomposition of nitrogen expanded austenite.<sup>[27]</sup>

#### 4.2. Development of carbides

The occurrence of iron-based Hägg carbide,  $M_5C_2$  is clearly related to a carbon content exceeding a critical concentration. For the carburizing temperatures 465 and 470°C the development of carbides (Hägg,  $Fe_3C$  and  $M_7C_3$ ) is likely to be related to the sudden increase in uptake at carbon contents of around 5-6 wt%. Hence the occurrence of Hägg carbide is not a consequence of the thermal exposure and associated (thermal) decomposition of carbon expanded austenite, but is a consequence of *exceeding* the maximum (metastable) solubility of carbon in expanded austenite. It is anticipated that the developing Hägg carbide has the same metallic composition as the starting alloy. This behavior is also fully consistent with the *in situ* observations of thermal decomposition where expanded austenite is gradually transformed into Hägg carbide. The carbides  $Fe_3C$  and  $M_7C_3$ , where M is mainly Cr, can be considered as decomposition products of Hägg carbide. These carbides were only observed for the highest carburizing temperatures applied, where partitioning of metallic elements would be possible on a limited scale.

To further verify this transformation sequence, part of the carburized powder sample used for the *in situ* investigation was rapidly heated to 600°C instead of a slowly increasing temperature. As seen in Figure 7, this caused a full transformation of the original expanded austenite, ferrite and Hägg carbide to austenite (with little or no carbon content) and  $M_7C_3$ .

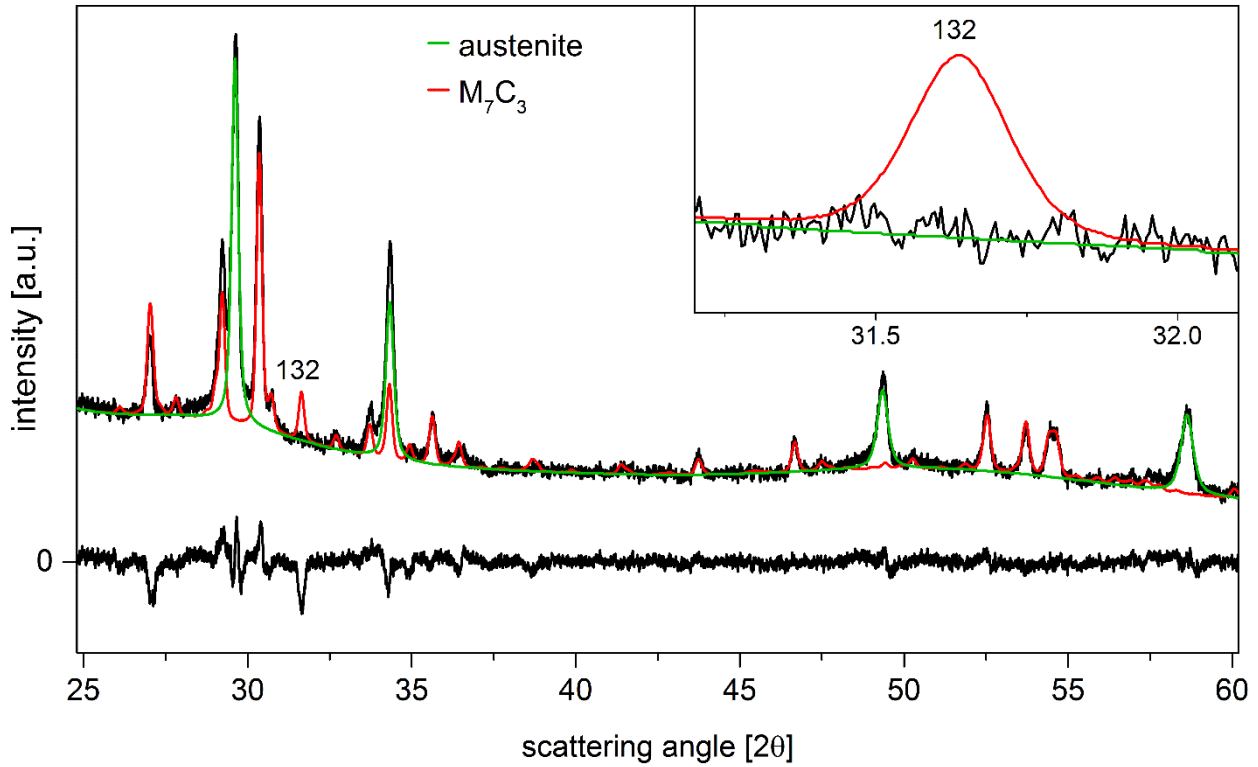


**Figure 7.** Synchrotron powder diffraction ( $\lambda = 1.07051(2) \text{ \AA}$ ) and Rietveld profiles for carburized  $5 \text{ }\mu\text{m}$  powder thermally decomposed at  $600 \text{ }^{\circ}\text{C}$ ; constituents are austenite and  $\text{M}_7\text{C}_3$  carbide. The inset shows the position of the extinct 132 reflection for  $\text{M}_7\text{C}_3$ .

For the  $\text{M}_7\text{C}_3$  carbide, the structural description reported by Fruchart & Rouault<sup>[28]</sup> was adopted; orthorhombic in space group  $Pnma$ . The 132 peak predicted for this structure is, however, not observed in the diffractogram (Figure 7), which may be explained by a partially disordered structure. The correct orthorhombic crystal structure is obtained at high temperature, but  $\text{M}_7\text{C}_3$  carbides prepared below  $1200^{\circ}\text{C}$  exhibit crystal imperfections due to formation of twins and stacking faults, resulting in broadening and disappearance of certain diffraction peaks.<sup>[29]</sup> This includes the 132 peak (or 321 for the  $Pm\bar{c}n$  setting used in the cited paper) and results in a “poorly crystallized” low-temperature structure indexed according to a hexagonal lattice. For the present data neither the hexagonal description in space group  $P63mc$ <sup>[30]</sup> nor the trigonal description in space group  $P31c$ <sup>[31]</sup> improved the fit since these predict additional peaks that were not observed. Consequently, the orthorhombic description was maintained and no indications of additional carbides were observed. The stable carbide at sufficiently high carbon content and temperature is thus  $\text{M}_7\text{C}_3$ , which is formed as a decomposition product from Hägg carbide. The fact that full

transformation is obtained at 600°C in contrast to the experiment with multiple temperature steps can be explained by an initial overshoot in temperature due to the rapid heating rate.

In the low temperature regime (420-380°C in Figure 2) the derivative of the uptake curve (end part) decreases continuously. It is speculated that this regime is associated with the continuous formation/precipitation of Hägg carbide within expanded austenite. When Hägg carbide develops/precipitates, expanded austenite is depleted in carbon, which is compensated by renewed carbon uptake. The capacity for carbon in Hägg carbide (C to M ratio of 0.4) is higher than for carbon in expanded austenite (an occupancy  $y_C$  or the equivalent C to M ratio of approximately 0.2). Consequently, the rate of carbon uptake reflects the rate of Hägg carbide development by nucleation and growth. The development of Hägg carbide with a high capacity for carbon, compared to the expanded austenite, may entail local carbon gradients in the expanded austenite; indeed variations in carbon content were observed as reflected by the asymmetrically broadened expanded austenite Bragg peaks (Figure 5 & Table 3). The presence of delta ferrite and the possible transformation into tetragonally distorted ferrite, which eventually may transform into expanded austenite, can also lead to local carbon gradients.

The observation that Hägg carbide occurs rapidly (within hours) can be explained as follows. Through-carburizing of the foils/powder takes place rapidly and homogenization and carbon build-up occurs much faster than for a bulk material. For bulk material the surface concentration of carbon is the outcome of a competition between the continued inward diffusive flux of carbon and the carbon flux provided through the surface (dissociation) reaction. If the flux of C atoms provided by the surface reaction is not infinitely large as compared to the flux of diffusion of carbon removed by solid state diffusion, no local (imposed) equilibrium is achieved at the surface, and the carbon content is lower than corresponding to local equilibrium. On saturation of the sample the

inward flux of carbon is reduced, leading to an increase of the surface concentration, promoting the development of Hägg carbide.

It has been observed by Cao et al.<sup>[11]</sup> that Hägg carbide can form with a composition similar to the alloy composition, which means that Ni and Fe are accommodated in the carbide structure. The present results strongly corroborate that no Ni partitioning occurs on forming Hägg carbide, as this would not be possible within reasonable time at a temperature as low as 380°C. Hence, it is suggested that para-equilibrium occurs between expanded austenite and Hägg carbide during the development of the latter. This implies that the relative contents of substitutionally dissolved elements in both phases are equal and deviate from the equilibrium compositions for (expanded) austenite and Hägg carbide while equilibrium for the carbon contents in both phases does prevail.

#### **4.3. Technological aspects**

For the system of nitrogen expanded austenite there exists a broad homogeneity range and even for a nitriding potential of infinity nitrogen expanded austenite is obtained. This is evidently not the case for the system of carbon expanded austenite, which has some clear technological repercussions. Applying low temperature carburizing of stainless steel the carbon potential or carbon activity has to be controlled in order to avoid unwanted precipitation of Hägg carbide and subsequently  $M_7C_3$  which occur when exceeding a threshold value in the expanded austenite, irrespective of temperature. Development of (surface) carbides may be detrimental for the corrosion resistance of stainless steel if they involve retraction of Cr atoms from solid solution and Cr is no longer available for maintenance of the protective oxide layer. The formation of iron rich carbide,  $Fe_3C$  is also unwanted in a stainless steel, with respect to corrosion resistance. Furthermore, the maximum solubility of  $y_C \approx 0.2$  in expanded austenite also implies a maximum hardening effect, which is a direct consequence of the amount of carbon in solid solution (solid solution hardening). For lower temperatures, e.g. below 420°C, the formation of  $M_7C_3$  does not take place, only the

formation of Hägg carbide. Hence, the formed Hägg carbide has ostensibly the same relative composition of substitutional elements as the alloy, which effectively means that Cr is not retracted from the austenite phase. The consequences of this with respect to electrochemical and mechanical properties need to be investigated.

## 5. Conclusions

In the investigated carburizing temperature interval (380 up to 470°C) metastable equilibrium between an imposed gas atmosphere and AISI 316 stainless steel is not attainable; all applied carburizing conditions resulted in carbides concomitantly with carbon expanded austenite. The maximum obtainable carbon content in expanded austenite, based on lattice expansion, was estimated as  $y_C=0.220$  (4.74 wt.%) at 380°C. Large amounts of Hägg carbide  $M_5C_2$  were observed with synchrotron diffraction analysis, irrespective of carburizing temperature and gas atmosphere; in the temperature range 465-470°C development of the carbides  $M_7C_3$  and  $Fe_3C$  also occurred. The formation of Hägg carbide appears to be directly correlated to the carbon concentration (in expanded austenite). Hägg carbide appears to develop by a transformation of expanded austenite, which does not entail partitioning of substitutional elements, i.e. perhaps as a para-equilibrium between carbide and expanded austenite. It is suggested that  $M_7C_3$  and  $Fe_3C$  form from the decomposition of Hägg carbide and involve partitioning of Fe, Cr and Ni atoms on prolonged carburizing treatment. In-situ thermal decomposition analysis by controlled temperature ramping in inert atmosphere confirms that expanded austenite is gradually transformed into Hägg carbide, which later decomposes into  $M_7C_3$ .

## Acknowledgements

Financial support from the Danish Research Council for Independent Research Technology and Production Sciences under grant no. 274-07-0344 and no. 11-106293 is gratefully acknowledged.

The authors are grateful to DANSCATT for financing the measurement stay at the MAX-VI laboratory.

## References:

- 
- [1] T. Christiansen, M.A.J. Somers Surface Engineering **2005**, 21, 445.
  - [2] S. Collins, P. Williams, Adv. Materials & Processes, September **2006**, 32.
  - [3] Edited by T. Bell and K. Akamatsu: Stainless Steel 2000 - Proc. 1st Int. Conf. on ‘Thermochemical Surface Engineering of Stainless Steel’, Osaka, Japan, November **2000**, Maney Publishing.
  - [4] US6461448, P.C. Williams, S.V. Marcx, **2002**, US patent.
  - [5] H. Dong, International Materials Rev. **2010**, 55(2), 65.
  - [6] J. Oddershede, T.L. Christiansen, K. Ståhl, M.A.J. Somers, Steel Research Int. **2012**, 83(2), 162.
  - [7] J. Oddershede, T.L. Christiansen, K. Ståhl, M.A.J. Somers, Scripta Mater. **2010**, 62, 290.
  - [8] G.M. Michal, F.Ernst, A.H. Heuer, Metall. Mater. Trans. A, **2006**, 37A, 1819.
  - [9] T.S. Hummelshøj, T.L. Christiansen, M.A.J. Somers, Scripta Mater. **2010**, 63, 761.
  - [10] Y.Sun, X.Li, T. Bell, Mater. Sci. and Technol., **1999**, 15(10), 1171.
  - [11] Y. Cao, F. Ernst, G.M. Michal, Acta Mater. **2003**, 51, 4171.
  - [12] F.Ernst, Y. Cao, G.M. Michal, Acta Mater. **2004**, 52, 1469.
  - [13] K. Farrell, E.D. Specht, J. Pang, L.R. Walker, A. Rar, J.R. Mayotte, J. Nucl. Mater. **2005**, 343, 123.
  - [14] F. Ernst, Y. Cao, G.M. Michal, A.H. Heuer, Acta Mater. **2007**, 55, 1895.
  - [15] H.E. du Plessis, J. P. R. de Villiers, G. J. Kruger, Z. Kristallogr. 2007, 222, 211
  - [16] T. Christiansen, M.A.J. Somers, Metall. Mater. Trans. A 2006, 37, 675.
  - [17] M.A.J. Somers, T. Christiansen, P. Møller, European patent EP1521861, **2003**.
  - [18] T.L. Christiansen, T.S. Hummelshøj, M.A.J. Somers, Surf. Eng. **2011**, 27(8), 602.
  - [19] K. Ståhl, J. Appl. Cryst., **2000**, 33(2), 394.

- 
- [20] C.J. Howard, R.J. Hill, AAEC (now ANSTO) Report M112, Lucas Heights Research Laboratory, **1986**.
- [21] F.H. Herbstein, J. Smuts, Acta Crystallogr. **1964**, 17, 1331.
- [22] H.E. du Plessis, J.P.R. de Villiers, G.J. Kruger, A. Steuwer, M. Brunelli, J. Synchrotron Radiat. **2011**, 18, 266.
- [23] J.P. Bouchard, Annales de Chimie, **1967**, 1967, 353
- [24] A.L. Bowman, G.P. Arnold, E.K. Storms, N.G. Nereson, Acta Crystallogr. B, **1972**, 28 3102.
- [25] H.J. Grabke, Arch. Eisenhüttenwes. **1975**, 46, 75.
- [26] T. Christiansen, M.A.J. Somers: Z. Metallkd, **2006**, 97, 79.
- [27] B. Brink, K. Ståhl, T.L. Christiansen, M.A.J. Somers, J. Appl Cryst. **2014**, 47(3), 819.
- [28] R. Fruchart, A. Rouault: Ann. Chim. (Paris), **1969**, 4, 143.
- [29] A. Rouault, P. Herpin, R. Fruchart: Ann. Chim. (Paris), **1970**, 5, 461.
- [30] F.H. Herbstein, J.A. Snyman: Inorg. Chem., **1964**, 6, 894.
- [31] A. Westgren: Jernkontorets Ann., **1935**, 118, 231.